nature geoscience

SUPPLEMENTARY INFORMATION

DOI: 10.1038/NGEO1292

Equatoiral winds on Saturn and the Stratospheric Oscillation

Liming Li[1*], Xun Jiang[1], Andrew P. Ingersoll[2], Anthony D. Del Genio[3], Carolyn C. Porco[4], Robert A. West[5], Ashwin R. Vasavada[5], Shawn P. Ewald[2], Barney J. Conrath[6], Peter J. Gierasch[6], Amy A. Simon-Miller[7], Conor A. Nixon[8], Richard K. Achterberg[8], Glenn S. Orton[5], Leigh N. Fletcher[9], Kevin H. Baines[5]

[1] *Department of Earth and Atmospheric Sciences, University of Houston, Houston, TX, USA.*

[2] *Division of Geological and Planetary Sciences, Caltech, Pasadena, CA, USA.*

[3] *NASA Goddard Institute for Space Studies, New York, NY, USA.*

[4] *CICLOPS/Space Science Institute, Boulder, CO, USA.*

[5] *Jet Propulsion Laboratory, Caltech, Pasadena, CA, USA.*

[6] *Department of Astronomy, Cornell University, Ithaca, NY, USA.*

[7] *NASA Goddard Space Flight Center, Greenbelt, MD, USA.*

[8] *Department of Astronomy, University of Maryland, College Park, MD, USA.*

[9] *Atmospheric, Oceanic and Planetary Physics, University of Oxford, Oxford, UK*

DOI: 10.1038/NGEO1292

Cassini Data Processing

1. Selection and Processing of ISS Multi-filter Images

There are thousands of ISS multi-filter images between 2004 and 2009 that cover the equatorial region of Saturn. In order to obtain accurate measurements of zonal winds in the equatorial region, we select the ISS images by several criteria in this study. Firstly, we focus on the southern equatorial region (0-20°S) of Saturn because this region has been observed since 2004. The northern equatorial region (0-20°N) is not discussed because most of the region was not clearly observed by ISS until 2009 due to the occultation/scattering of rings. Secondly, we only select high-resolution ISS image pairs with relatively long time separation to decrease the uncertainty of wind measurements. The selected ISS image pairs, which have high spatial resolution and long time separation, are described in Table S1.

Table S1. ISS Multi-Filter Images Used in This Study

Date	Sub-solar Latitude (Solar Longitude)	Camera	Filter	Wavelength	Spatial Resolution
May 10, 2004	24.8°S (291.0°)	NAC	MT3/CB3	938/889 nm	162 km/pixel
Dec. 30, 2008	3.4°S (352.3°)	WAC	MT3/CB3	938/889 nm	69 km/pixel

Note: The ISS images taken on May 10 of 2004 are a pair of images separated by 20.5 hours (~ two Saturn rotations) at the filters MT3 and CB3, respectively. The ISS images taken on December 30 of 2008 are a pair of images separated by 9.6 hours. The CB3 images were taken 42 seconds after the corresponding MT3 images, which makes them virtually simultaneous. The resolution presented here is the spatial resolution of the raw ISS images, which is different from

the spatial resolution of the cylindrical maps in the text. Solar longitude is defined as the longitude of the Sun on the sky with the zero of longitude at northern spring equinox.

The processing of ISS images includes navigation, photometric calibration, and map projection. The procedures of navigation and photometric calibration are standard, based on the camera geometric model and the photometric calibration software (CISSCAL)[1] and the Navigation and Ancillary Information Facility (NAIF) at the Jet Propulsion Laboratory[2], respectively. The map projection is cylindrical (rectangular) with equal increments of latitude and longitude by considering the geometry of the equatorial region. These relatively standard procedures of navigation, calibration, and projection have already been described and used in some of our previous studies[2,3,4,5]. It should be emphasized that the removal of the solar illumination in the equatorial region of Saturn requires careful treatment because of the complex scattered sunlight from rings. Here, we combine an approach with a high-pass filter with a box size 7.5°×7.5°, which was developed in the previous study[2], and the classical Minnaert function[6], to remove the solar illumination from the raw ISS images in the equatorial region of Saturn.

2. Introduction of CIRS Observations and Corresponding Thermal Winds.

The selected CIRS observations, which are close to the corresponding ISS observations, are described in Table S2.

Table S2. CIRS Nadir Retrieved Temperature Maps of Saturn Used in This Study

Date	Solar Longitude	Emission Angle	Coverage	Spatial Resolution (y and z)
Apr. 8, 2005	303.3°	0-75°	85°S– 0°	1° and ~ 1 scale height
Dec. 29, 2008	352.2°	0-74°	89°S– 0°	1° and ~ 1 scale height

DOI: 10.1038/NGEO1292

Note: CIRS nadir observations with high spatial resolution in the horizontal plane are used in this study. The retrieved zonal-mean temperature in the plane containing both the meridional coordinate (y) and altitude (z) has the highest spatial resolution in the meridional direction, which is critical for the integration of thermal winds[5].

The CIRS instrument and the temperature retrieval are described in detail elsewhere[7,8], and used extensively in our previous studies[5,9-11]. The retrieved temperature maps in the plane of latitude (0-20°S) and pressure (1-500 mbar) are based on CIRS observations in focal planes FP1 (300-500 mbar), FP3 (50-300 mbar), and FP4 (1-5 mbar), as discussed in the literature[11]. There is no information between 5 and 50 mbar, so that region is removed when doing the integration of thermal winds[5].

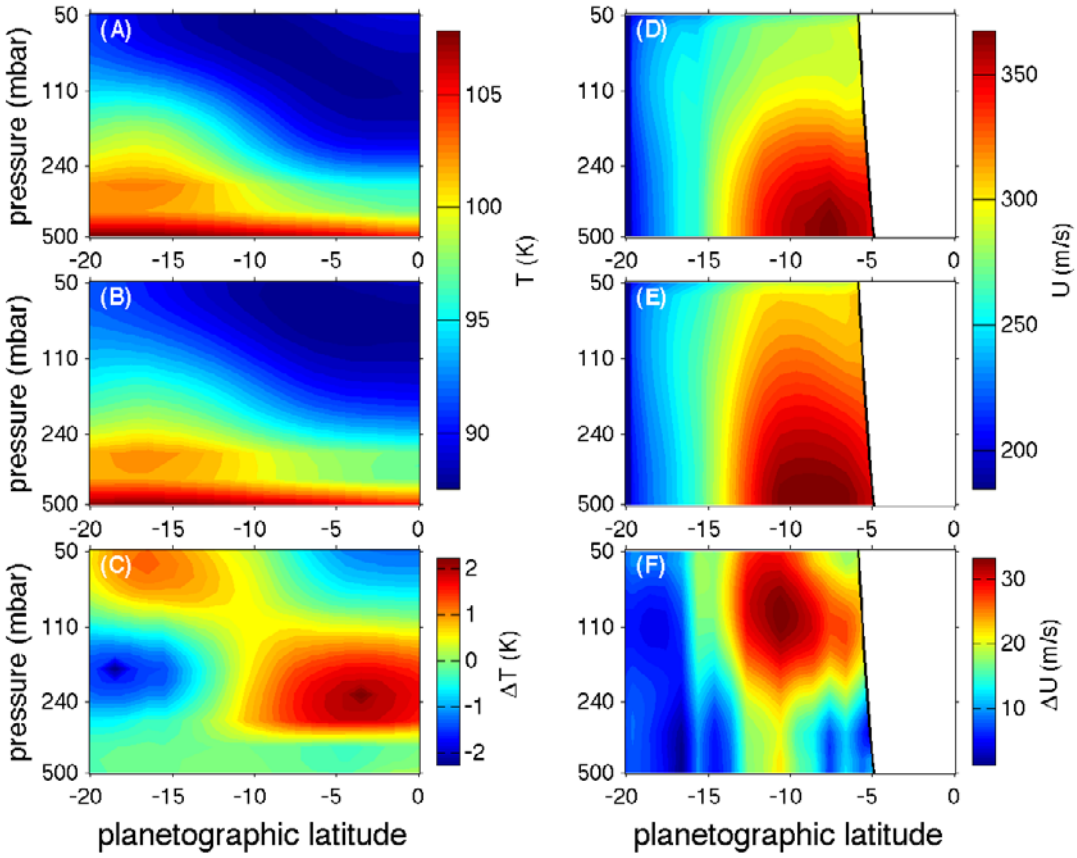

Figure S1. Temperatures and thermal winds in the equatorial troposphere of Saturn. (A) CIRS retrieved temperature in 2005. (B) CIRS retrieved temperature in 2008. (C) Temperature difference between 2005 and 2008. (D) Thermal winds in 2005. Zonal winds at the boundary layer (500 mbar) are taken from the ISS winds at the filter CB3 in 2004 and 2008 for the CIRS thermal winds in 2005 and 2008, respectively. The black line is the cylindrical integration routine of our modified thermal wind equation[5]. (E) Thermal winds in 2008. (F) Difference of thermal winds between 2005 and 2008.

Figure S1 shows the thermal winds in the troposphere (50-500 mbar) of Saturn, which are based on the CIRS retrieved temperature and our modified thermal wind equation[5]. Instead of using the combined zonal winds from Voyager and Cassini at the cloud deck as the zonal winds at the boundary level (i.e., 500 mbar) for the vertical integration in our previous study[5], we use the measured winds from the ISS CB3 images as the zonal winds at the boundary level to keep the rough consistence in time between the boundary condition and the CIRS temperature. The profile of thermal winds at 60 mbar, which is used in Fig. 1 in the main text, is taken from this figure.

Figure 2S shows the thermal winds in the stratosphere (1-5 mbar) of Saturn based on the CIRS nadir observations. In the region near the equator (0-10°S), the atmospheric temperature increased ~ 3 K below 2-mbar and decreased ~ 3 K above 2-mbar. These changes occurred from 2005 to 2008 when Saturn was approaching Spring equinox. The magnitude of temperature variation is larger than the uncertainty of the CIRS retrieved temperature (~ 1 K).

DOI: 10.1038/NGEO1292

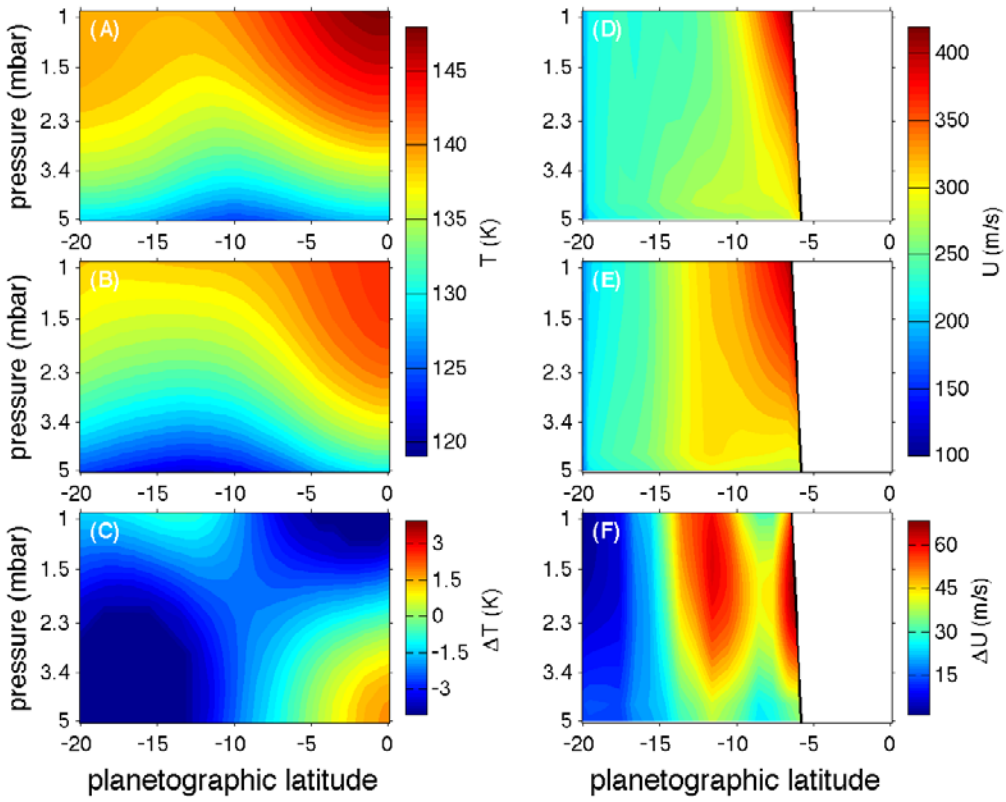

Figure S2. Temperature and thermal winds in the equatorial stratosphere of Saturn. (A) CIRS retrieved temperature in 2005. (B) CIRS retrieved temperature in 2008. (C) Temperature difference between 2005 and 2008. (D) Thermal winds in 2005, which correspond to the temperature in 2005 (A). Zonal winds at the boundary layer (5 mbar) are taken from the winds at the top level of Fig. S1 by assuming that there is no significant variation of zonal winds between 5 and 50 mbar, where the CIRS nadir observations have no spectral sensitivity there. The black line is the cylindrical integration routine of our modified thermal wind equation. The region very close to the equator is left blank because of the lack of zonal winds within 0-5°S at the boundary layer and the integration routine of our modified thermal wind equation. (E) Thermal winds in 2008. (F) Difference of thermal winds between 2005 and 2008.

3. Analysis of Uncertainty of Wind Measurements Based on ISS Images.

The uncertainty of wind measurements, which are based on the ISS images, is discussed in this section. The first possible uncertainty is related to the reference frame for the wind measurements, which is based on the rotation period of Saturn, and may possibly vary with time[12-13]. However, any potential variation of rotation period over a relatively long time scale does not affect the temporal variation of zonal winds, which are measured on a consistent reference. The second possible source of uncertainty is the navigation procedure. In general, the navigation of ISS images, which is conducted by fitting the observed planetary limb to its predicted location, has a precision smaller than one pixel. The procedure introduces small systematic errors due to imprecise knowledge of the altitude of limb-defining opacity. The ISS images used in this study were navigated by using the same portion of the planetary limb, so the possible systematic errors occur in the same direction. Such errors are mitigated by the relative wind measurements conducted in this study. Therefore, we argue that the navigation procedure does not introduce significant uncertainty to the wind measurements based on ISS images.

After excluding the possible uncertainty from the varying rotation period and the navigation procedure, the uncertainty of cloud-tracking winds based on ISS images are estimated by adding the following three sources: i) the standard deviation of multiple wind measurements within each 1° latitude bin; ii) the uncertainty related to the full width at half maximum (FWHM) of the point spread function (PSF) of the ISS cameras[1,4]; and iii) the uncertainty related to locating of cloud/haze features in the ISS images. The first uncertainty (i.e., standard deviation of wind measurements) is a few meters per second. The FWHM of the PSF is 1.3 pixels and 1.8 pixels for the Narrow Angle Camera (NAC) and Wide Angle Camera (WAC)[1], respectively.

DOI: 10.1038/NGEO1292

Most of the cloud features used in the cloud-tracking method have sizes of a few pixels. Here, we simply assume that the uncertainty related to the locating of cloud features is ~ 1 pixel. Combining the second and third sources, we have the uncertainty as ~ 2.3 pixels and ~ 2.8 pixels for NAC and WAC, respectively. The time separation between the pair of images selected in this study (Table S1) is ~ 10 hours. The spatial resolution of the cylindrical ISS maps is ~105 km/pixel at the equator (Fig. 1). At this resolution, the uncertainty of winds related to the second and third sources is 6.7 m/s and 8.2 m/s for cloud-track wind measurements based on the NAC and WAC images, respectively. Adding the three sources together, we have the uncertainty of cloud-track wind measurements, which is shown as horizontal solid lines in Fig. 2. For the uncertainty of correlation wind measurements, only the second source (FWHM of PSF) is considered, which is 3.8 m/s and 5.2 m/s for the correlation wind measurements based on the NAC and WAC images, respectively. Such uncertainty is shown as horizontal dashed lines in Fig. 2.

References

1. Porco, C. C. *et al*. Cassini Imaging Science: Instrument characteristics and anticipated scientific investigations at Saturn. *Space Sci. Rev.* **115**, 363-497 (2004).

2. Vasavada, A. R., Horst, S. M., Kennedy, M. R., Ingersoll, A. P., Porco, C. C., Del Genio, A. D. & West, R. A. Cassini imaging of Saturn: southern hemisphere winds and vortices. *J. Geophy. Res.* **111**, E05004 (2006).

3. Porco, C. C. *et al*. Cassini imaging science: Initial results on Saturn's atmosphere. *Science* **307**, 1243-1247 (2005).

4. Li, L., Ingersoll, A. P., Vasavada, A. R., Simon-Miller, A. A., Del Genio, A. D., Ewald, S. P., Porco, C. C. & West, R. A. Vertical wind shear on Jupiter from Cassini images, *J. Geophy. Res.* **111**, E04004 (2006).

5. Li, L., Gierasch, P. J., Achterberg, R. K., Conrath, B. J., Flasar, F. M., Vasavada, A. R., Ingersoll, A. P., Banfield, D., Simon-Miller, A. A. & Fletcher L. N. Strong jet and a new thermal wave in Saturn's equatorial stratosphere. *Geophys. Res. Lett.* **35**, L23208 (2008).

6. Minnaert, M. The reciprocity principle in lunar photometry. *Astrophys. J.* **93**, 403-410 (1941).

7. Conrath, B. J., Gierasch, P. J., Ustinov, E. A. Thermal structure and para hydrogen fraction on the outer planets from Voyager IRIS measurements, *Icarus* **135**, 501-517 (1998).

8. Flasar, F. M. *et al*. Exploring the Saturn system in the thermal infrared: the composite infrared spectrometer. *Space Sci. Rev.* **115**, 169-297 (2004).

9. Flasar, F. M. *et al*. Temperatures, winds, and composition in the saturnian system. *Science* **307**, 1247-1251 (2005).

DOI: 10.1038/NGEO1292

10. Fletcher, L. N., Irwin, P. G. J., Teanby, N. A., Orton, G. S., Parrish, P. D., de Kok, R., Howett, C., Calcutt, S. B., Bowles, N. & Taylor, F. W. Characterizing Saturn's vertical temperature structure from Cassini/CIRS. *Icarus* **189**, 457-478 (2007).

11. Fletcher, L. N., Achterberg, R. K., Greathouse, T. K., Orton, G. S., Conrath, B. J., Simon-Miller, A. A., Guerlet, S., Irwin, P. G. J. & Flasar, F. M. Seasonal Change on Saturn from Cassini/CIRS Observations, 2004-2009. *Icarus* **208**, 337-352 (2010).

12. Gurnett, D. A., Persoon, A. M., Kurth, W. S., Groene, J. B., Averkamp, T. F., Dougherty, M. K. & Southwood, D. J. The variable rotation period of the inner region of Saturn's plasma disk. *Science* **316**, 442-445 (2007).

13. Anderson, J. D. & Schubert, G. Saturn's gravitational field, internal rotation, and interior structure. *Science* **317**, 1384-1387 (2007).